Journal of Applied Electrochemistry (2005) 35:751–756
DOI 10.1007/s10800-005-1618-7

Synthesis of metal–cadmium sulfide nanocomposites using jingle-bell-shaped core-shell photocatalyst particles

BONAMALI PAL[1], TSUKASA TORIMOTO[1,2,3], KENTARO IWASAKI[3], TAMAKI SHIBAYAMA[4], HEISHICHIRO TAKAHASHI[4] and BUNSHO OHTANI[2,3,*]
[1]*"Light and Control", PRESTO, Japan Science and Technology Agency, 4-1-8 Honcho Kawaguchi, Saitama, Japan*
[2]*Catalysis Research Center, Hokkaido University, Sapporo, 001-0021, Japan*
[3]*Graduate School of Environmental Earth Science, Hokkaido University, Sapporo, 060-0811, Japan*
[4]*Center for Advanced Research of Energy Technology, Hokkaido University, Sapporo, 060-8628, Japan*
*(*author for correspondence, e-mail: ohtani@cat.hokudai.ac.jp; phone: +81-11-706-9132; fax: +81-11-706-9133)*

Received 1 July 2004; accepted in revised form 2 September 2004

Key words: cadmium sulfide, core-shell particle, gold, jingle bell structure, nanoparticle, photocatalyst, photodeposition, silver, size-selective photoetching

Abstract

Photocatalytic deposition of gold (Au) and silver (Ag) nanoparticles was investigated using jingle-bell-shaped silica (SiO_2)-coated cadmium sulfide (CdS) nanoparticles (SiO_2/CdS), which each had a void space between the CdS core and SiO_2 shell, as a photocatalyst. A size-selective photoetching technique was used to prepare the jingle bell nanostructure of SiO_2/CdS. Nanoparticles of Au and Ag were deposited by irradiation of the photoetched SiO_2/CdS in the presence of the corresponding metal complexes under deaerated conditions. Chemical etching of Au-deposited particles enabled the selective removal of CdS without any influence on the surface-plasmon absorption of Au. TEM analyses of the resulting particles suggested that some particles were encapsulated in hollow SiO_2 particles, while other Au particles were deposited on the outer surface of the SiO_2 shell. Emission spectra of the photoetched SiO_2/CdS showed that the metal deposition developed a broad emission with a peak around 650 nm originating from surface defect sites, the degree being dependent on the kind of metal nanoparticles and their amount of deposition. This fact can be explained by the formation of metal–CdS binary nanoparticles having defect sites at the interface between metal and CdS.

1. Introduction

Several synthetic methods have been used to obtain a surface coverage of nanoparticles of either metals or semiconductors in a core-shell morphology in order to modify physical and chemical properties of the core materials without their coagulation into larger particles [1–7]. For example, a silica shell layer was prepared by polymerization/precipitation of silane compounds on the particle surface [1–4], and a shell composed of polyelectrolytes and charged nanoparticles was prepared by layer-by-layer deposition on the core surface [8]. Furthermore, the partial removal of core materials in core-shell particles has been reported to result in the formation of the novel structures, such as metal or semiconductor nanoparticles-encapsulated hollow spheres that had void space between the core and shell [9–15]. These particles have attracted much attention because the void spaces are expected to be suitable for novel catalytic reactions and for the fabrication of a nanostructure.

We have recently developed a novel strategy to control the size of a cadmium sulfide (CdS) core in a core-shell morphology [16–18]. The application of size-selective photoetching to silica (SiO_2)-coated CdS (SiO_2/CdS) nanoparticles enabled selective decrease of CdS core size, resulting in the formation of void spaces between the CdS core and the SiO_2 shell (a nanosized "jingle bell"). The size of the void space could be controlled from 1.4 to 2.4 nm by adjusting the wavelength of monochromatic irradiation for CdS photoetching from 514 to 458 nm [16]. One of the significant features is that the photoetched CdS cores had exposed bare surfaces and their surrounding SiO_2 shells were sufficiently porous for small ionic species such as Cd^{2+} and OH^- to penetrate from the bulk solution to the interior of the SiO_2 shell [18]. Therefore, the photoetched CdS cores behave like bare particles suspended in a solution phase even if they are incorporated in hollow SiO_2 particles. This feature alone enables us to change the physicochemical properties of the size-quantized

CdS nanoparticles without mutual coalescence by modifying the bare surface of CdS core with different materials such as metal or semiconductor particles.

In this study we prepared the metal–semiconductor nanocomposites through photocatalytic reaction by SiO_2/CdS particles and investigated the influence of metal loading on the photochemical properties of CdS core particles. Irradiation of photoetched CdS induced photocatalytic deposition of gold (Au) and silver (Ag) nanoparticles both inside the void spaces of jingle-bell-shaped SiO_2/CdS nanoparticles and on their outer surfaces. Subsequent chemical etching of CdS cores gave metal nanoparticle-encapsulated hollow SiO_2 particles having jingle-bell structures. The emission property of SiO_2/CdS changed significantly depending on the kind of metal and on the amount of its deposition.

2. Experimental section

2.1. *Materials*

Sodium bis(2-ethylhexyl)sulfosuccinate (AOT), 1,1′-dimethyl-4,4′-bipyridinium dichloride (methylviologen, MV^{2+}), and 3-mercaptopropyltrimethoxysilane (MPTS) were purchased from Tokyo Chemical Industry. Cadmium perchlorate (Kishida Reagents Chemicals) and potassium dicyanogold(I) ($KAu(CN)_2$, Nacalai Tesque) were used as received. Other chemicals were supplied from Wako Pure Chemical Industries. Aqueous solutions were prepared just before use with water purified by a Yamato/Millipore WP501 Milli-Q system.

2.2. *Size-selective photoetching of silica-coated cadmium sulfide (SiO_2/CdS) nanoparticles*

Silica (SiO_2)-coated cadmium sulfide (CdS) nanoparticles were prepared using the AOT-reversed-micelle method as reported previously [17, 19]. Size-selective photoetching was applied to the thus-obtained particles to prepare jingle bell nanostructures. SiO_2/CdS powder (80 mg) was suspended in 50 cm^3 of oxygen-saturated water containing 50 μmol dm^{-3} MV^{2+} and irradiated with monochromatic light until its diffuse reflectance spectra had become unchanged (typically for 8 h). Irradiation of monochromatic light at 488 nm was performed using an argon-ion laser (Ion Laser Technology, model 5500A) with intensities of ca. 60 mW, respectively. The powders were washed with water and methanol several times and dried under vacuum.

2.3. *Photochemical deposition of gold (Au) or silver (Ag) nanoparticles onto SiO_2/CdS*

The jingle-bell-shaped SiO_2/CdS nanoparticles were re-suspended in aqueous methanol (50 vol%) containing $KAu(CN)_2$ or potassium dicyanosilver(I) ($KAg(CN)_2$) and irradiated at >300 nm by a 400 W high-pressure mercury arc lamp typically for 1.5 h under an argon atmosphere. The resulting powder was isolated by centrifugation and washed with water and methanol, followed by drying under vacuum. The powder was suspended in diluted sulfuric acid (0.1 mol dm^{-3}) and stirred for 96 h to dissolve CdS selectively, when necessary.

2.4. *Characterization*

For the measurement of diffuse reflectance spectra, sample powders were diluted with barium sulfate powder to give a content of 1 wt% and measured in a dry state using a photonic multi-channel analyzer (Hamamatsu Photonics, PMA-11) and pure barium sulfate as a reference. Emission spectra were recorded on a fluorescence spectrometer (Shimadzu RF-5300PC) with excitation wavelength at 350 nm. SiO_2/CdS powders (1.5 mg) were suspended in water (1.5 cm^3) and poured into a quartz cell. The suspension was vigorously stirred during the emission measurement. The structure and size distribution of photodeposited Au nanoparticles were examined by using a JEOL 2010F transmission electron microscope (TEM) with an acceleration voltage of 200 kV. TEM samples were prepared by dropping the powder suspension onto a copper grid covered with amorphous carbon overlayers (Ouken Shoji, type B) and drying under vacuum.

3. Results and discussion

3.1. *Photodeposition of gold nanoparticles*

Figure 1 shows the changes in diffuse reflectance spectra of SiO_2/CdS. Original particles exhibited an absorption onset at ca. 550 nm. Since the energy gap of bulk CdS has been reported to be 2.4 eV [20] (corresponding to the absorption onset of ca. 520 nm), most of the CdS nanoparticles had an energy gap similar to that of the bulk materials. Monochromatic irradiation at 488 nm caused its blue shift to ca. 490 nm. This indicates that the CdS core in SiO_2/CdS was successfully photoetched to the size expected from the wavelength of irradiation light, resulting in the formation of a void space between the CdS core and SiO_2 shell as reported previously [16]. When the photoetched SiO_2/CdS powders were irradiated in the presence of the gold complex under deaerated conditions, a new broad absorption band assignable to a surface plasmon (SP) band of Au particles [21–23] appeared in the range of wavelengths longer than 500 nm. Irradiation for more than 1.5 h caused almost no change in the diffuse reflectance spectra, indicating that the photodeposition of Au nanoparticles was completed within 1.5 h. It should be noted that a marked decrease in CdS absorption in the wavelength range of 300–500 nm was observed by the deposition of Au. Similar phenomena have been reported for Ag-deposited spherical ZnO nanoparticles [24], CdS-capped Au nanoparticles [25], and

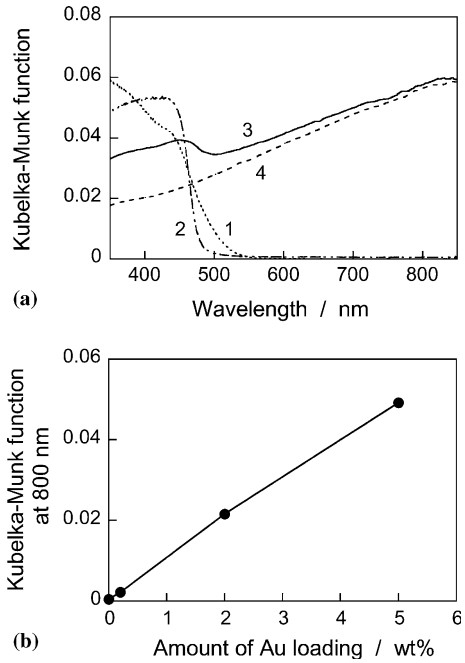

Fig. 1. (a) Diffuse reflectance spectra of various SiO_2/CdS samples: (1) original, (2) after photoetching at 488-nm laser light irradiation, (3) after 5 wt% Au photodeposition, and (4) after chemical etching of CdS. (b) Intensity of the SP peak of Au as a function of amount of Au loading.

Au-deposited CdSe nanorods [26], where the changes in the absorption band of semiconductor particles were most likely induced by the electronic interaction between the metal and semiconductor particles. Therefore, the observation of the decrease in the exciton band indicated that the Au nanoparticles were deposited directly on the surface of CdS nanoparticles, resulting in the formation of metal-semiconductor binary particles (i.e. Au–CdS) incorporated in the SiO_2 shell (SiO_2/CdS–Au), as conceptually shown in Scheme 1. Furthermore, when the amount of Au loading was increased, the intensity of the SP band increased linearly without changes in the spectral shape up to at least 5 wt% Au loading, as shown in Figure 1b.

The absorption assigned to CdS nanoparticles in SiO_2/CdS–Au disappeared following chemical treatment with diluted sulfuric acid, suggesting the formation of SiO_2/Au. The resulting powders had an SP band position of Au nanoparticles similar to that of the corresponding SiO_2/CdS–Au. TEM images of these

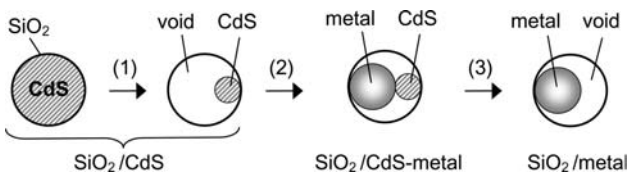

Scheme 1. Schematic illustration of photodeposition of metal nanoparticles on SiO_2/CdS and its chemical etching. The procedures used in this process were size-selective photoetching (1), photodeposition (2), and chemical etching (3).

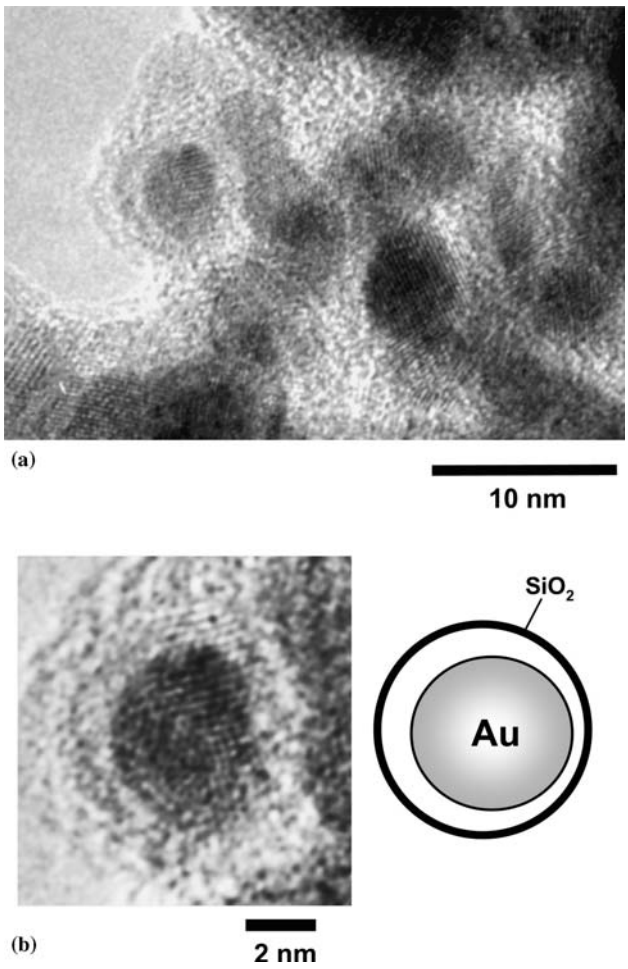

Fig. 2. TEM images of Au nanoparticles incorporated in SiO_2 shells. Image (b) is a high magnification image of a particle shown in image (a). A schematic illustration of the structure is also shown.

particles are shown in Figure 2. We could not obtain clear evidence in TEM images of connection between CdS and Au in SiO_2/CdS–Au due to the overlapping of particles. The complete removal of CdS was confirmed by EDX analyses. Almost spherical Au nanoparticles were observed in the aggregation. A high magnification image of a particle (Figure 2b) clearly shows that Au nanoparticles had lattice fringes with interplanar spacing of 0.20 nm assigned to the (200) lattice plane of the face-centered cubic structure of a gold crystal [27]. Furthermore it was clearly seen in the image shown in Figure 2b that an Au nanoparticle with a size of ca. 4 nm was surrounded by an SiO_2 hollow shell (with a size of ca. 6 nm), a jingle bell structure, as depicted in the schematic illustration. The void space between the Au core and SiO_2 shell was calculated to be ca. 2 nm from the size difference between the Au nanoparticle and the hollow SiO_2 particle. Consequently, Au nanoparticles were photodeposited in the void space of jingle-bell-shaped SiO_2/CdS and the surrounding SiO_2 shell prevented coalescence of the Au nanoparticles during the chemical treatment. However, the average size (d_{av}) of the CdS core photoetched at 488 nm was determined by TEM observation to be 3.4 nm with

standard deviation (σ) of 0.40 nm, which was larger than the void space in SiO_2/Au observed in Figure 2b. A possible explanation for this difference is change in the shape of the Au deposits; the deposition must occur to cover the CdS surface, but the Au deposits might transform into spherical particles of least surface energy during and/or after the CdS dissolution. The total volume of particles with diameters of 3.4 nm (CdS) and 4 nm (Au) does not exceed the volume of the inner space of hollow SiO_2 (6 nm).

The size distribution of Au nanoparticles was obtained by measuring the sizes of more than 80 particles in TEM images, as shown in Figure 3. The Au nanoparticles had a broad size distribution with d_{av} of 7.6 nm and σ of 2.2 nm. The original CdS nanoparticles had sizes in the range 3.5–7 nm with d_{av} of 5.0 nm and σ of 0.79 nm, and the inner diameter of SiO_2 was equal to the diameter of CdS before photoetching as reported previously [16]. Thus, it seems reasonable to assume that the photodeposited Au nanoparticles had sizes less than ca. 7 nm. However, this was not the case; the sizes of many of the Au nanoparticles were in the range of 7–14 nm. The photodeposition of Au nanoparticles might occur on the outer surface of the SiO_2 shell as well as inside the void space. This possibility was supported by the results of photodeposition of Au using original SiO_2/CdS as a photocatalyst: a broad SP band of Au nanoparticles appeared in the range of wavelengths longer than 500 nm with irradiation. The SiO_2 shell thickness was estimated to be ca. 0.3 nm from elemental analyses of original SiO_2/CdS. Since original particles had no void space inside the SiO_2 shell, this fact indicated that the shell was thin enough to induce electron transfer through it and to drive the photodeposition on the outer surface of the SiO_2 shell.

The photoadsorption properties of Au nanoparticles deposited in the jingle-bell-shaped particles were compared with those of single-component Au nanoparticles with similar particle size. It is well known that spherical Au nanoparticles homogeneously dispersed in an aqueous solution exhibit a sharp absorption peak assigned to the SP band at about 520 nm, the peak position is almost independent of the particle size in the range from 8 to 60 nm [23, 28]. Therefore, Au particles obtained in the present study, which had the sizes in this range, would exhibit the sharp SP peak at around 520 nm, but, in practice, only a broad absorption band appeared in the range of wavelengths longer than 500 nm, as shown in Figure 1a. Mulvaney and co-workers have reported, in their study of particulate films composed of 13-nm-Au nanoparticle encapsulated in SiO_2 spheres, that the SP peak position was remarkably red-shifted along with decrease in the interparticle spacing due to enhanced dipole–dipole interaction between Au nanoparticles [21, 22]. Therefore, it is probable that the shell thickness of the present jingle-bell-shaped SiO_2/CdS particles, 0.3 nm in average, is small enough to red-shift the SP peak of photodeposited Au nanoparticles.

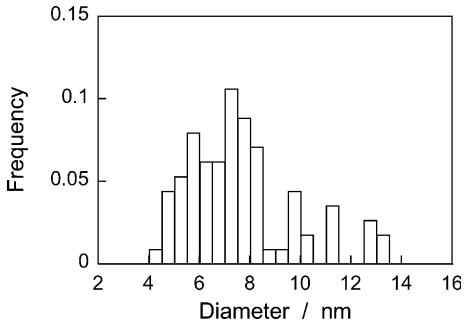

Fig. 3. Size distribution of Au nanoparticles obtained from TEM images.

3.2. *Photodeposition of silver nanoparticles*

Figure 4 shows the changes in diffuse reflectance spectra of SiO_2/CdS particles before and after 0.5 wt% Ag deposition. The irradiation of the original or photoetched particles caused the appearance of a broad absorption around 600 nm assigned to the SP band of Ag nanoparticles, suggesting that the Ag nanoparticles were also photodeposited both on the outer surface and inside the void space of the SiO_2 shell. However, the observed peak position was red-shifted from that of Ag colloid for a spherical particle, ca. 400 nm, in the size between 10 and 27 nm [23, 29]. Assuming the photodepositied Ag nanoparticles in photoetched SiO_2/CdS similar to that of Au nanoparticles (Figure 3), the

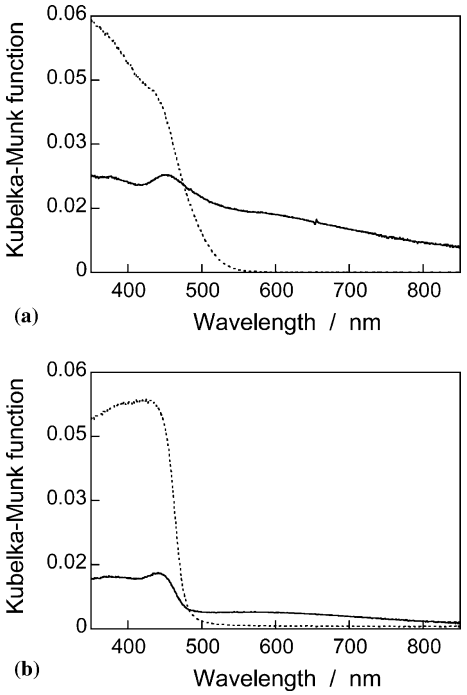

Fig. 4. Diffuse reflectance spectra of SiO_2/CdS particles before (dotted lines) and after 0.5 wt% Ag deposition (solid lines). SiO_2/CdS particles used were original particles (a) and those photoetched with 488-nm irradiation (b).

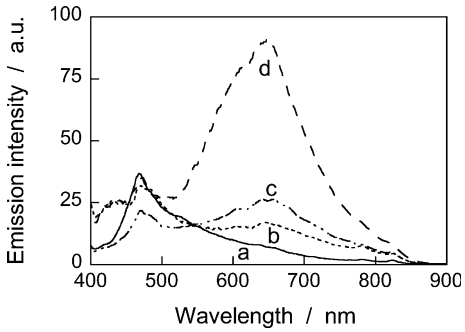

Fig. 5. Emission spectra of 488 nm-photoetched SiO_2/CdS powders. Samples were those obtained before (a) and after metal photodeposition of 0.2 wt% Au (b), 5.0 wt% Au (c), and 0.5 wt% Ag (d). The excitation wavelength was 350 nm.

observed red-shift of SP band may originate from the above-mentioned dipole–dipole interactions between metal nanoparticles [22]. Furthermore, it should be noted that the absorption onset of SiO_2/CdS photoetched at 488 nm was almost the same regardless of the Ag photodeposition, indicating that the CdS size also changed negligibly during the Ag nanoparticle deposition under deaerated conditions. The intensity of the exciton peak of CdS nanoparticles was diminished by the deposition of Ag as observed in the Au photodeposition on SiO_2/CdS, suggesting that Ag nanoparticles were photodeposited directly on the CdS surface and then Ag and CdS core particles interacted electronically with each other.

3.3. *Emission properties of metal-loaded SiO_2/CdS*

Figure 5 shows the emission spectra of 488 nm-photoetched SiO_2/CdS powders before and after metal photodeposition. The photoetched SiO_2/CdS without metal deposition exhibited band gap emission at 468 nm, while broad emission appeared from metal-deposited samples in the wavelength range of 500–800 nm with a peak around 650 nm, which was attributed to the recombination of photogenerated charge carriers at surface defect sites in CdS nanoparticles [30, 31]. The emission intensity was greatly dependent on the kind of metal nanoparticles and their amount. With an increase in the amount of Au deposited, the emission originating from the surface defect sites was enhanced, while the band gap emission became small. The photodeposition of Ag nanoparticles considerably enhanced the emission at 650 nm compared to that observed for Au deposition. These results show that the metal nanoparticles deposited on the surfaces of CdS cores, i.e., Au–CdS or Ag–CdS binary nanoparticles in hollow SiO_2 particles, produced surface defect sites at the interface between the CdS core and metal nanoparticles, the degree being dependent on the kind of metal nanoparticle. Although the details are ambiguous at present, difference in the dispersibility of metal particles and/or in the electronic interaction between CdS and metal particles may account for this difference in emission properties.

4. Conclusion

The void space of the jingle-bell-shaped SiO_2/CdS has been shown to work as a reaction space for metal photodeposition. The removal of CdS by chemical etching enabled the preparation of Au-encapsulated hollow SiO_2 particles (SiO_2/Au). The emission property of the photoetched CdS in the jingle bell structure was modified by the formation of a metal-semiconductor binary structure, the degree of modification depending on the kind of metal and its amount. Since metal deposition on the outer surface of the SiO_2 shell could not be prevented due to the electron transfer through the thin shell layer, selective preparation of metal–semiconductor binary nanoparticles incorporated in an SiO_2 shell or metal-encapsulated SiO_2 hollow particles could not be achieved in the present study. It should be possible to deposit metal nanoparticles on a desired site in the jingle-bell-shaped SiO_2/CdS by changing the SiO_2 shell morphology such as thickness and coverage. Study along these lines is currently in progress.

Acknowledgements

This research was partially supported by a Grant-in-Aid for Scientific Research (B) (No. 16350095) from the Japan Society for the Promotion of Science and by a Grant-in-Aid for Scientific Research on Priority Areas (417) (No. 14050043) from the Ministry of Education, Culture, Sports, Science and Technology (MEXT) of Japan.

References

1. S.Y. Chang, L. Liu and S.A. Asher, *J. Am. Chem. Soc.* **116** (1994) 6745.
2. S.Y. Chang, L. Liu and S.A. Asher, *J. Am. Chem. Soc.* **116** (1994) 6739.
3. P. Mulvaney, L.M. Liz-Marzan, M. Giersig and T. Ung, *J. Mater. Chem.* **10** (2000) 1259.
4. L.M. Liz-Marzan and P. Mulvaney, *J. Phys. Chem. B* **107** (2003) 7312.
5. F. Caruso, *Adv. Mater.* **13** (2001) 11.
6. D. Gerion, F. Pinaud, S.C. Williams, W.J. Parak, D. Zanchet, S. Weiss and A.P. Alivisatos, *J. Phys. Chem. B* **105** (2001) 8861.
7. A. Schroedter, H. Weller, R. Eritja, W.E. Ford and J.M. Wessels, *Nano Lett.* **2** (2002) 1363.
8. F. Caruso, *Chem.-Eur. J.* **6** (2000) 413.
9. M. Giersig, L.M. Liz-Marzan, T. Ung, D.S. Su and P. Mulvaney, *Ber. Bunsen-Ges. Phys. Chem.* **101** (1997) 1617.
10. M. Giersig, T. Ung, L.M. LizMarzan and P. Mulvaney, *Adv. Mater.* **9** (1997) 570.
11. M. Kim, K. Sohn, H. Bin Na and T. Hyeon, *Nano Lett.* **2** (2002) 1383.
12. J.Y. Kim, S.B. Yoon and J.S. Yu, *Chem. Commun.* (2003) 790.
13. K. Kamata, Y. Lu and Y.N. Xia, *J. Am. Chem. Soc.* **125** (2003) 2384.
14. K.T. Lee, Y.S. Jung and S.M. Oh, *J. Am. Chem. Soc.* **125** (2003) 5652.
15. T. Inomata and K. Konishi, *Chem. Commun.* (2003) 1282.

16. T. Torimoto, J.P. Reyes, K. Iwasaki, B. Pal, T. Shibayama, K. Sugawara, H. Takahashi and B. Ohtani, *J. Am. Chem. Soc.* **125** (2003) 316.
17. T. Torimoto, J.P. Reyes, S.Y. Murakami, B. Pal and B. Ohtani, *J. Photochem. Photobiol. A: Chem.* **160** (2003) 69.
18. K. Iwasaki, T. Torimoto, T. Shibayama, H. Takahashi B. Ohtani, *J. Phys. Chem. B* **108** (2004) 11946.
19. B. Pal, T. Torimoto, S. Ikeda, T. Shibayama, K. Sugawara, H. Takahashi and B. Ohtani, *Top. Catal.* in press.
20. Y.V. Pleskov and Y.Y. Gurevich, *Semiconductor Photoelectrochemistry* (Consultants Bureau, New York, 1986).
21. T. Ung, L.M. Liz-Marzan and P. Mulvaney, *J. Phys. Chem. B* **105** (2001) 3441.
22. V. Salgueirino-Maceira, F. Caruso and L.M. Liz-Marzan, *J. Phys. Chem. B* **107** (2003) 10990.
23. D.L. Feldheim and C.A.J. Foss, *Metal Nanoparticles* (Marcel Dekker Inc., New York, 2002).
24. S.H. Chen and U. Nickel, *Chem. Commun.* (1996) 133.
25. P.V. Kamat and B. Shanghavi, *J. Phys. Chem. B* **101** (1997) 7675.
26. T. Mokari, E. Rothenberg, I. Popov, R. Costi and U. Banin, *Science* **304** (2004) 1787.
27. Powder Diffraction File (JCPDS International Center for Diffraction Data, 1982), No.4–0784.
28. J.H. Hodak, A. Henglein and G.V. Hartland, *J. Chem. Phys.* **111** (1999) 8613.
29. H. Nabika and S. Deki, *J. Phys. Chem. B* **107** (2003) 9161.
30. U. Resch, A. Eychmueller, M. Haase and H. Weller, *Langmuir* **8** (1992) 2215.
31. L. Spanhel, M. Haase, H. Weller and A. Henglein, *J. Am. Chem. Soc.* **109** (1987) 5649.